Biochimica et Biophysica Acta, 1108 (1992) 159–168

BBAMEM 75693

Cooperative gating of chloride channel subunits in endothelial cells

Alain Queyroy and Jean Verdetti

Groupe d'Electrophysiologie Moléculaire, Laboratoire de Physiologie et Pathologie Cellulaire, Université Joseph Fourier, Grenoble (France)

(Received 10 March 1992)

Key words: Patch-clamp; Chloride channel; Endothelial cell; Cooperative gating

New methods are described to detect subconductance levels and to analyse ion channel gating. These methods are applied to simulated and experimental data. Single chloride channel records from inside-out membrane patches excised from human umbilical veinous endothelial cells (HUVEC) exhibit, in addition to the full closed and full open configurations, intermediate subconductance levels which are multiple of an elementary conductance of 112.5 pS. Analysis of transitions from one state to another and the comparison of real data with simulated data leads to the proposal of a cooperative model of gating for the observed subunits of a chloride channel.

Introduction

Ion channels are large integral membrane proteins which control the passive flux of ions through lipid cell membranes [1] by switching between closed and open conformations that permit this flow. The patch-clamp technique [2] enables one to perform current recording of the flow of ions through ion channels.

Ion channel gating mechanisms have been generally assumed as Markovian processes with a small number of open and closed channel states. However, other ion channel gating models have been developed in terms of non Markovian processes as fractal [3] diffusion and reptation models [4,5]. Furthermore, recently, it has been demonstrated that a deterministic model of ion channel gating based on the theory of chaotic process can mimic an intrinsic random process [6]. In this model, the current through the channel at time $(t + dt)$ is a function of the value of the current at the previous time (t). Nevertheless, comparative studies of Markovian, fractal, diffusion and related models of ion channel gating provide justification for continued to use of Markovian models in the exploration of channel gating mechanisms [7–9]. However, the validity of Markovian models and classical mathematical methods used to study Markovian signals have been questioned [6,10].

Correspondence to: A. Queyroy, Groupe d'Electrophysiologie Moléculaire, Laboratoire de Physiologie et Pathologie Cellulaire, Université Joseph Fourier, BP 53X 38 041, Grenoble cedex, France.

Based on patch-clamp recording, three different conducting states of a channel can be predicted. Firstly, current through a channel is minimal and thus the channel is closed. Secondly, current through the channel is maximal and the channel is fully open. For the third state, when the channel switches between these open and closed states, the current passes through certain levels corresponding to subconductance states. For the subconductances two types of gating have been described [11]. The first type is called 'subunit' and the second 'partially open' (or partially closed) substate. Subunit gating is indicated when the conductance of a channel changes with steps of equal value. Those kinds of substate have been described for chloride channels [12,13]. The second type of substate has been observed for several channels: potassium channels [14–16], chloride channels [17]. Nevertheless, it is not demonstrated whether subconductance states represent a partially open channel or whether they result from the presence of parallel conductive units as shown for potassium channels in renal tubules [18]. On the other hand, it has been observed that, sometimes, open channel currents are separated from each other by short closed periods called flickers. Such flickers exhibiting subconductance levels have been described for nicotinic ion channels [19].

Furthermore, related or not to subconductance states, it has been shown, for Na conductance in squid axon, that disparities exist between the micro- and macro-kinetics [20] and that channel interactions can be observed [21–23]. These observations suggest that

linear models are not always appropriate for to describe the gating of the channels. Thus, it has been proposed that the kinetic model for allosteric enzymes can be considered as an alternative model of gating [24].

Many parameters are used to characterize a channel. Conductance is one of them. It is usually estimated from the slope of the current-voltage relationship. To build this relationship, the most frequent method consists in using data provided by binned histograms of current amplitude measurements for different membrane potential values. In such histograms, each current level is represented by a Gaussian population. Unfortunately, only main current levels can be distinguished by this method especially when the signal/noise ratio is low or when the baseline is distorted. Furthermore, there is no automatic method to detect transient subconductance states so, a time-consuming visual inspection is the only method used. Thus, to overcome this difficulty, some authors [16] have built two types of amplitude histograms ('raw' and 'excluded') from the same long period of uninterrupted current recording. Nevertheless, the direct inspection of records of digitalized data remains the most applied method. Yet, when they are observed, subconductance states are difficult to be incorporated into channel gating models and are frequently disregarded. However, the great variety and the large number of ion channels which exhibits substates demonstrate the importance of this mechanism for the physiology of the cell (for review see Ref. 11).

In the present study, we describe an alternate approach to the analysis of patch-clamp records containing transient substates of conductance. The procedure is verified using simulated ion channel data. Its application is illustrated using data from the chloride channels of human umbilical veinous endothelial cells (HUVEC). These channels exhibit multi-current levels which can be described by four subunits exhibiting a cooperative mode of gating.

Materials and Methods

Isolation of endothelial cells

Human umbilical veinous endothelial cells were obtained according to the method of Jaffé [25]. Briefly, the cells were isolated in a medium (M 199 Boehringer Mannheim) containing 0.5 unit/ml of collagenase type IA (Sigma). Then the cells were plated at 10^5 cells/ml density on fibronectin coated dishes (Falcon) and cultured in M 199 medium supplemented with 30% pooled human serum, 100 U/ml penicillin, 0.1 mg/ml streptomycin and 2 mM glutamine. The cells were incubated at 37°C in humidified 5% CO_2/95% O_2 atmosphere. Cells grow to confluence after 5 to 7 days. Cells from passage 3–4 were used in these experiments.

Current measurement

Standard patch-clamp technique was used [2]. Patch pipettes were made from Kimax-51 glass capillaries (Kimble Products) and filled with extracellular solution containing: 110 mM Cl TEA buffered at pH 7.35 by 10 mM Hepes. The pipette resistances were 3–5 Mohms. The recordings were made in the 'inside-out' patch configuration, with a symmetrical bathing solution. The current signal was obtained by using a patch-clamp amplifier (RK 300 Biologic, Claix, France), sampled at 8 kHz. Data were analysed on a Tandon PCA/12 microcomputer using a commercial software (Biopatch, Biologic, Claix, France) and a program developed in our laboratory.

Data analysis

Transition detection. We have developed an automatic computerized program to detect transitions in long lasting patch-clamp records. The procedure is based on the scanning of the record by a detecting running window. The amplitude range and the duration range of the window are chosen by the operator on the basis of the signal characteristics (sampling rate, signal/noise ratio). The choice of the operator is made easier by signal and analysis window displaying. In this program, the event finder subroutine is different from that of the Event-Catching Program proposed by Sigworth [26]. A single-channel signal is considered as a succession of steady state and transient state sections. A steady state section is a record section where current values are close to a mean value. On the other hand, a transient section is a record section where the current values exhibit a deviation higher than the standard deviation. During the scanning of the record by the running window, steady state and transient state sections of the record are detected. If points exhibit an amplitude dispersion lower than the amplitude range of the window, they are considered as the components of a steady state section and the current amplitude value of each point is considered as equal to the mean value. The other sections are classed as transient sections. A specific procedure is used to analyze these sections. In this procedure, the variation of the current amplitude between two consecutive points of the transition is calculated and compared to the standard deviation. If this amplitude is equal to, or greater than the standard deviation no transition is detected. For the subsequent histogram the coefficient of this point is considered as zero. On the other hand, when this amplitude is equal to zero a transition is detected and, for the subsequent histogram, the coefficient of these points is assumed to be one. Finally, when the current amplitude between two points varies from zero to the standard deviation, the corresponding points are affected with a coefficient varying in a proportional manner between one and zero. Furthermore, a time thresh-

old is utilized to detect the events exhibiting a duration less than a chosen value (which can be determined according to the bandwidth of the amplifier and the filter characteristics).

Current amplitude histograms. In a theoretical signal (Figs. 1a and 1b), different types of current level can be distinguished: long lasting current levels called steady-state current levels and short lasting current levels called transient state current levels. Therefore, three types of current histograms can be built: (i) a 'classical' current level amplitude histogram (Fig. 1c); (ii) a current step histogram corresponding to the current variation between two consecutive steady-state current levels [26]; (iii) a current step histogram corresponding to variation of current from a steady state to the following transient states (Fig. 1d).

Signal reconstitution and baseline distortion removal. Using the data obtained from the running window detection and from the current step histograms, the ideal ion channel signal can be identified. For this purpose, each experimental point is classified as baseline or as a state of open channel. This classification is based on the comparison of each experimental data with the value of current steps given by the current

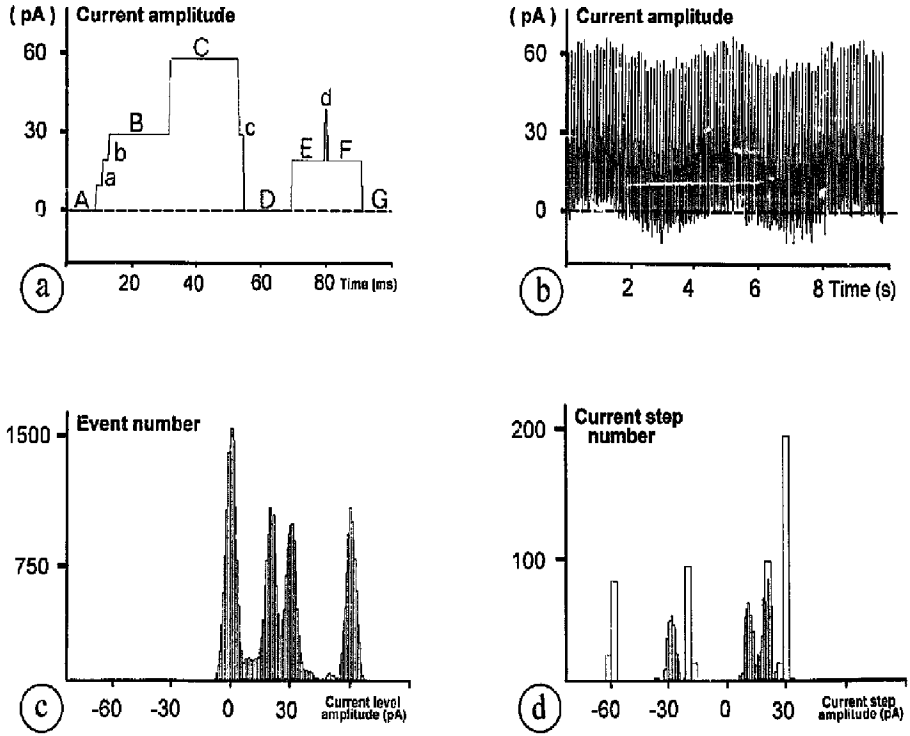

Fig. 1. Simulated ion channel signal data analysis. (a) Signal from of an elementary sequence generated by an external simulator (SMP 300, Biologic, Claix, France). A, B, C, D, E, F and G are long-lasting current levels (duration more than 10 ms).; a, b, c are short lasting intermediate levels (duration: 2 ms), d is a flicker (duration: 1 ms). (b) In this simulated signal, the elementary sequence described in Fig. 1a has been repeated a hundred times, the baseline has been distorded by addition of $i = 5\sin(1\pi t/4F)+\sin(2\pi t/F)$ function (t, time in ms; F, sampling frequency in Hz; i, current in pA), a Gaussian noise with a standard deviation of 3 pA, coming from a real record, has been then added. (c) Classic level histogram performed from the simulated signal shown on Fig. 1b. Using the Biopatch software (Biologic, Claix, France), the baseline distortion has been removed, the gaussian peaks correspond to the main current levels, respectively, (A + D + G) for 0 pA, (b + E + F) for 20 pA, (B + c) for 30 pA and C for 60 pA. Short lasting current levels (a) and (d) cannot be distinguished in this histogram. The (b) and (c) steps are masked, respectively, by (E + F) and (B) main current levels. (d) Current steps histogram performed on the values of the simulated signal shown in Fig. 1b, without any previous baseline distortion removal. White bins represents current variations from one steady state to another: (−60 pA: C → D; −20 pA: F → G; 20 pA: D → E; 30 pA: A → B and B → C). Dark bins represent current variations from a steady state to the following transient states (−30 pA: C → c; 10 pA: A → a; 20 pA: A → b and E → d).

step histogram. Thus, each experimental data point corresponding to a step of current is substituted for the most likely ideal value. When no step is detected, current level is considered as equal to the previous value, thus the baseline distortion is automatically removed and an idealized signal is built.

Event map. Data from a single-channel record consists in switches from one current level to another. Using the idealized signal, a map representing the signal as a $di = f(i)$ function can be built (Fig. 2). In this map, each event is plotted with previous current level (i) as abscissa and current step amplitude (di) as ordinate. Plot surface is proportional to event number. As defined before, some events are too short and thus are considered as unresolved. Therefore, the number of transient states or flickers exhibiting too short a duration, less than a fixed time threshold, are plotted on the abscissa-axis and are not taken into account.

Simulated signals. To test the ability of our program to detect short lasting events, we have built a signal exhibiting short lasting events, a low signal/noise ratio and a baseline distortion. For this purpose we have used a stimulator (SMP300, Biologic, Claix, France), giving the elementary sequence of the signal shown in Fig. 1a. This sequence was repeated one hundred times. Then the baseline was distorded using the function:

$$i = 5\sin(2\pi t/4F) + \sin(2\pi t/F)$$

where i is the current amplitude (pA), F is the sample frequency (Hz) and t is the time (ms). Furthermore, a Gaussian noise coming from a real record with a standard deviation equal to 3 pA has been added (Fig. 1b).

Gating of simulated subunit signal. To model the signal observed with chloride channels of HUVEC, we have synthesized two types of simulated signals. Firstly, a signal resulting from the sum of four independent Markovian channels (or subunits), secondly, a signal resulting from the activity of two pairs of cooperative channels. In the first case, the opening constant rate was chosen equal to $10^{-2}\ s^{-1}$, and the closing constant rate to $7 \cdot 10^{-2}\ s^{-1}$. The general kinetics of each channel unit is described as follows:

$$(0\ pA)C \underset{7\cdot 10^{-2}\ s^{-1}}{\overset{10^{-2}\ s^{-1}}{\rightleftharpoons}} O(-4.5\ pA)$$

In the second case, channel gating already respects a Markovian process. However, in each couple, the channels are cooperative. Initial gating of one subunit

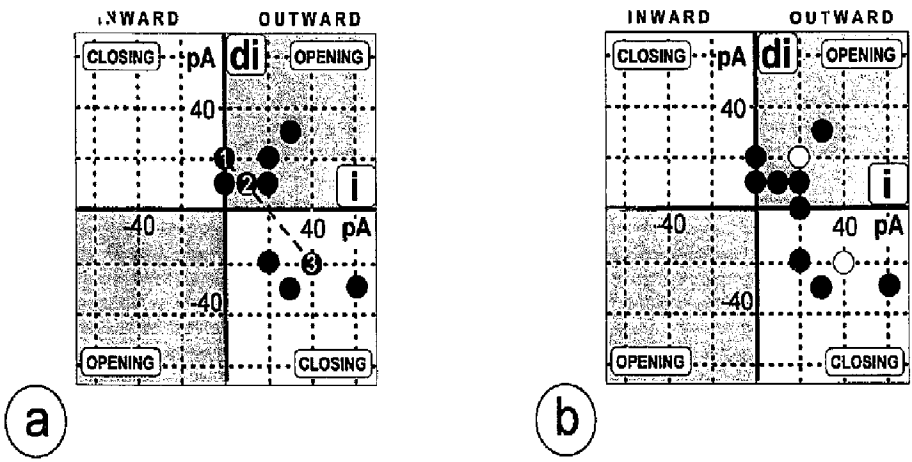

Fig. 2. Event map representation of simulated record. After a reconstitution of the signal in an ideal form, it is possible to map event gatings as a $di = f(i)$ function. This figure shows gating events of the simulated signal of Fig. 1a. In such a representation, each gating event is plotted with previous current level as abscissa (i) and current step amplitude as ordinate (di). The plot surface is proportional to the number of events. The baseline is represented by a central point (0;0). When the channels are opening (grey squares) inward currents are plotted in the bottom left hand corner and outward currents in the top right hand corner. When the channels are closing (white squares), inward currents are plotted in the top left hand corner and outward currents are plotted in the bottom right hand corner. (a) The time threshold is equal to 0 ms. In this case, every event is taken into account. This map can be used to determine the gating origin of the channel: for example, the diagonal alignement crossing the abscissa axis at 20 pA (dashed line) shows that the 20 pA current levels (b, E, and F) are reached after: (i) the opening of the full closed channel (D: 0 pA → E: 20 pA), plot No. 1 (0;20); (ii) the opening of the partial open channel (a: 10 pA → b: 20 pA), plot No. 2 (10;10); (iii) the closing from the 40 pA state (d: 40 pA → F: 20 pA), plot No. 3 (40; − 20) (The plot numbers appear as white digits within black circles.). (b) Event mapping of the same signal with a time threshold equal to 1.5 ms: opening and closing of 1 ms flickers (20 pA ↔ 40 pA), previously plotted, respectively, at (20;20) and (40; − 20) (white plots), are gathered as unresolved events on the abscissa axis (20;0).

triggers the gating of the other subunit (Fig. 4). A χ^2-test has been used to compare the simulated signals characteristics to those of the experimental record.

Results

Simulated data analysis

The behaviour of a complex channel exhibiting subconductance states and flickering have been simulated (Fig. 1a). By repeating this sequence a hundred times with the addition of Gaussian noise and the distortion of the basal level, a simulated single-channel record is obtained (Fig. 1b). Each elementary sequence includes a short lasting current (a, b, c) and flickers (d). As shown in Fig. 1c, the 'classical' current level amplitude histogram performed after the baseline distortion has been removed, shows only main current levels (0 pA for A, D and G; 20 pA for E and F, 30 pA for B and 60

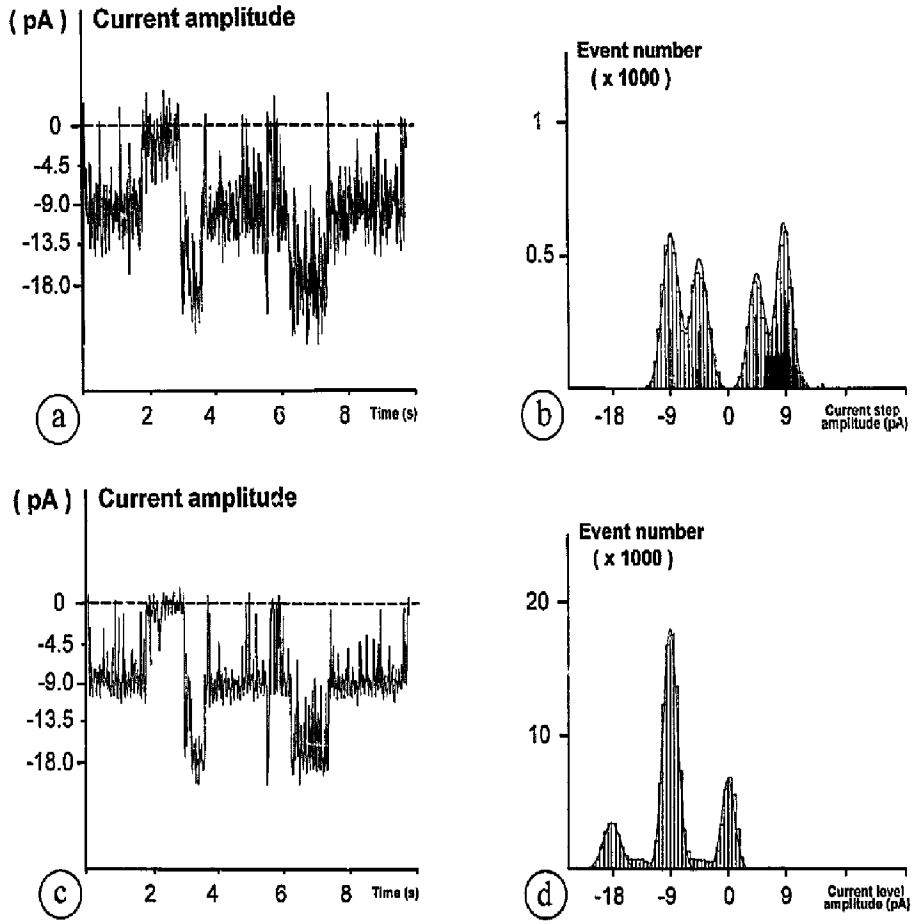

Fig. 3. Signal from chloride channels observed on an inside out patch of a human umbilical veinous endothelial cell with a membrane potential clamped at −40 mV. (a) Signal sampled at 8 kHz before filtering and baseline distortion removal (1/80 display). (b) Current step histogram of previous signal. White bins show steady state to steady state current steps, dark bins show steady state to following transient state current steps. A state is considered steady if it lasts more than 10 ms. Four types of gating can be observed: −4.5 and −9 pA current steps correspond to opening while 4.5 and 9 pA current steps correspond to closing. No current step of ±13.5 pA or ±18 pA is observed. This histogram leads to the conclusion of the existence of four elementary channels or subunits of −4.5 pA (112.5 pS). (c) Real signal of Fig. 3a after 500 Hz Hanning filtering and baseline smoothing correction (1/80 display). (d) Classical current level histogram performed on the filtred signal shown in Fig. 3c. In this histogram only three main current levels are shown at 0 pA (fully closed), −9 pA and −18 pA. No intermediate current level can be distinguished at −4.5 or −13.5 pA. Alone, this histogram leads to the conclusion of the existence of only two channels of −9 pA (225 pS).

pA for C). Transient substates (a, b, c) and flickers (d) cannot be distinguished. By contrast, using the computation procedure described in Materials and Methods, the histogram of current transitions performed on the steady current levels shows main current steps (C → D: −60 pA; F → G: −20 pA; D → E: 20 pA; A → B and B → C: 30 pA) while histogram of transitions from a steady state to a transient state shows transient events (C → c: −30 pA; A → a: 10 pA; A → b: 20 pA) (Fig. 1d). Furthermore, using the transition histograms this 'record' has been transformed into an idealized 'record' without any noise nor baseline distortion. The observed proportion of transitions from one level to another in the noisy and distorded simulated signal has been compared to the theoretical proportion of these transitions. The χ^2-test has shown ($P < 0.05$) that smoothing of the baseline and idealization of the signal do not induce any significant alteration of gating information and that the transitions are correctly detected. Using the data of this idealized record, we have built the event map shown in Fig. 2. The gating of the channel can be deduced from the observation of this map: thus, we can predict all transitions leading from an open state to another open state or leading from an open state to a closed state (and vice versa). According to the signal cut-off frequency, the operator can fix a time threshold under which transient events are disregarded (Fig. 2b).

Experimental data analysis

Vascular endothelial cells exhibit several types of ion channels: non selective cation channels [27], calcium channels [28], potassium channels [14,29], chloride channels [30]. Fig. 3a shows a typical inside-out-patch record of HUVEC chloride channels. Several intermediate conductance levels and flickers can be observed: the histogram of current steps (Fig. 3b) shows ±4.5 and ±9 pA current steps from one steady state to another (white bins) as well as from a steady state to a transient state (black bins). No current step of ±13.5 or ±18 pA is detected. After 500 Hz Hanning filtering and the removal of baseline distortion (Fig. 3c), a classical current level histogram can be constructed (Fig. 3d). On this histogram, three current levels can be identified 0 pA (baseline), −9 pA and −18 pA. No intermediate level is measurable either at −4.5 pA or at −13.5 pA.

Using the values given by the current step histograms (steps of ±4.5 and ±9 pA) the real signal of Fig. 3a has been idealized (Fig. 5-A1). A current level histogram performed with the values corresponding to this idealized signal points out the existence of five current levels: 0 pA, −4.5 pA, −9 pA, −13.5 pA and −18 pA (Fig. 5-A2).The distribution of current levels (Fig. 5-A2) is not binomial ($P < 0.05$). An event map representation (Fig. 5-A3) gives the gating of the channels. For example, it can be observed, that four pathways lead to the open state (9 pA level): (i) opening from 0 pA level (current step amplitude: −9 pA); (ii) opening from −4.5 pA level (current step amplitdue: −4.5 pA); (iii) closing from −13.5 pA level (current step amplitude: 4.5 pA); (iv) closing from −18 pA level (current step amplitude 9 pA).

Discussion

Ion channel behaviour can be interpreted by assuming that the channel exhibits two conductance states (open and closed) and that the transitions between these states can be described by a Markovian process. However, it has been noticed that many ion channels do not conform to this simple model and include subconductance states between the closed and the main open states: potassium channels [31,32], calcium channels [33], chloride channels [12,34]. Furthermore, it has been proposed that a channel would be expected to exhibit a continuum of many conformational states rather than few discrete states [35], [6].

Standard analysis of unit channel data are inefficient to detect very transient subconductance states (Fig. 1c) leading to the proposition of simple gating mechanisms. In this paper, we describe an improved method for the detection and analysis of ion channel subconductance states, which can be used to detect transient event such as intermediate steps and flickers. Furthermore, event mapping and utilization of models give informations on the complex behaviour of channels.

The 'classical' current amplitude histogram (Fig. 3d) applied to the analysis of HUVEC chloride channels shows only three current levels (0 pA, −9 pA and −18 pA), leading to the conclusion that this record results from the activity of two unitary channels of −9pA. By contrast, current step histograms (Fig. 3b) show the existence of steps of ±4.5 pA (112.5 pS). This current step value is an integral fraction of −9 and −18 pA, leading to the conclusion that there are four channels (or subunits) with current of −4.5 pA. In agreement with this observation, the current level histograms performed on the idealized signal disclose intermediate current levels of −4.5 and −13.5 pA (Fig. 5-A2). Occupancy of the different states by the chloride subunits deviates from a binomial distribution ($P < 0.05$) leading to the conclusion that the chloride channel subunits are not independent. Thus, it can be observed that levels 0 pA, 9 pA and −18 pA exhibit a larger probability of occupancy than −4.5 pA and −13.5 pA levels. Moreover, an event map (Fig. 5-A3) shows that simultaneous opening or closing is frequently observed between main states. For example: −9 pA current steps are often observed between 0 pA and −9 pA and between −9 pA and −18 pA, but rarely between −4.5

pA and −13.5 pA. If channels were independent the simultaneous opening or closing would obey a binomial distribution as shown on Fig. 5-B2. However, this is not the case, the simultaneous opening (or closing) of three and four subunits is too rare (Fig. 5-B3). Thus, as mentioned above, the chloride subunits are not independent. With a time threshold of 0.5 ms, −4.5 pA subunits are gating either singly or in pairs leading to the conclusion that a functionnal coupling exists between two units of the same two-channel cluster.

Some proteins are already known to be composed of multiple subunits. In some of them, the binding of a substrate to one subunit influences the binding of the substrate to the other subunit (ex: O_2/hemoglobin). This process is called cooperativity. In addition to cooperativity, a molecule exhibits allosteric interactions when its activity depend on the occupency of a binding site. The discrepancy observed between the micro- and macro-kinetics for Na conductance in squid axon [20], fluctuations and linear analysis of Na current kinetics in squid axon [36] and evidence of channel interaction [16,22,23,37,38] suggest that cooperative gating exists in ionic channels and that the application of the kinetic properties of allosteric proteins could be applicable to ion channels in membranes [24,39]. Thus, allosteric induction of channel conformation switches has been proposed to explain subconductance states observed in the acetylcholine nicotinic receptor channel [40,41], in calcium channels [42], and in potassium channels [33]. To test this hypothesis for chloride channels, we have built two simulated signals resulting from the activity of four Markovian subunits. Fig. 5-B1 shows a simulated signal built with four independent subunits as described in Materials and Methods. The closing rate constant is here more important than the opening rate constant. Consequently, low current levels (0 pA, −4.5 pA) are more frequent than high current levels (−9 pA, −18 pA). The occupancy probability of each current level fits a binomial distribution (Fig. 5-B2). Event mapping with a time threshold equal to 0.5 ms shows clearly that elementary openings are frequent (di = −4.5 pA) while simultaneous opening are rare. Thus, no simultaneous opening of four channels is observed (di = −18 pA), three simultaneous opening (di = −13.5 pA) is less frequent than two simultaneous opening (di = −9 pA). On the other hand, three simultaneous closing (di = 13.5 pA) are more frequent than two simultaneous closing (di = 9 pA). The event map of this signal built with four independent subunits (Fig. 5-B3) is statistically different ($P < 0.05$) from the real data (Fig. 5-A3). As the model of four independent subunits was unsuitable to describe the behaviour of the observed HUVEC chloride channels, we have built a gating model including a strong cooperativity in coupled subunits. This model is based on the concerted model proposed for allosteric protein by MONOD et al. [43]. We assume that: (i) observed channels exhibit the activity of two independent pairs of subunits; (ii) the subunits of each pair exhibit a concerted cooperativity; (iii) gating of each subunit conforms to a Markovian process. The final model includes four channels gathered into two clusters of two subunits. Opening of each subunit results in −4.5 pA current. With each pair of subunits in the fully closed state (CC), the rate constant of the initial gating of one subunit is low ($6 \cdot 10^{-4}$ s^{-1}), in return an initial gating of one subunit increases the rate constant of the other subunit up to 10^{-2} s^{-1}. In such a model the first subunit which opens (or closes) becomes a trigger for the other subunit. Nevertheless, the 'trigger subunit' can go back to its previous configuration before the gating of the other subunit, with a constant rate equal to $7 \cdot 10^{-2}$ s^{-1}. Thus the model, shown in Fig. 4, exhibits a positive cooperativity through an allosteric interaction between two unitary subunits. In each pair of subunits the cluster is in a stable state when the two subunits are in the same conformation (CC or OO) and in an unstable state when the two subunits are in opposite conformations (CO or OC). The signal simulated by

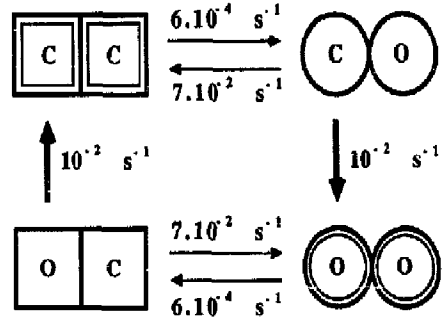

Fig. 4. Cooperative kinetic model to generate a simulated signal close to the observed signal of chloride channel from human umbilical veinous endothelial cells. To simulate the signal shown on Fig. 5-C1, two pairs of channels have been considered. In each pair of channels (or subunits) the gating probabilities of one element depend on its state as well as on the state of its neighbour. A state corresponds to a spatial conformation (open: O, closed C) and a kinetic potential (relax: square), (tense: circle). The pair of channels is in a stable state when the two channels are closed or open (double line) and in unstable states when one subunit is open and the other closed (single line). When the bisubunit is in a full closed state (CC), the opening probability of each subunit is equal to $6 \cdot 10^{-4}$ s^{-1}. When one subunit is open, its closing rate constant is $7 \cdot 10^{-2}$ s^{-1} while opening constant rate of its neighbour increases up to 10^{-2} s^{-1}. The opening of a subunit in a bisubunit includes, then, an initial opening which is a trigger for the second opening (CC ↔ OC → OO). The closing of a fully open bisubunit respects symetrical kinetics (OO ↔ OC → CC). Thus, in this simulated model, half-open states (OC) have not the same gating potentiality when it result from an initial opening (high opening rate constant) or when it result from a closing (high closing rate constant).

the addition of two couples of cooperative subunits (Fig. 5-C1) looks like the real one (Fig. 5-A1), this is confirmed by a χ^2-test performed on the current level histograms data corresponding to the Figs. 5-A2 and 5-C2, as well as by χ^2-test performed on the event maps data of Figs. 5-A3 and 5-C3, (Table I), ($P < 0.05$). As in experimental data, the simulated signal exhibit three main current levels (0 pA, −4.5 pA and −18 pA) and two intermediate sublevels (−4.5 and −13.5 pA), flickers are observed essentially at main current levels. The simultaneous opening of two subunits is observed at 0 pA and −9 pA ($di = -9$ pA), and simultaneous closing is observed at −18 and −9 pA ($di = 9$ pA). Finally the subunit behaviour in the simulated signal is closed to that of observed chloride channels. Therefore, it can be concluded that the cooperative model proposed for these HUVEC chloride channels, may be an appropriate model to describe the

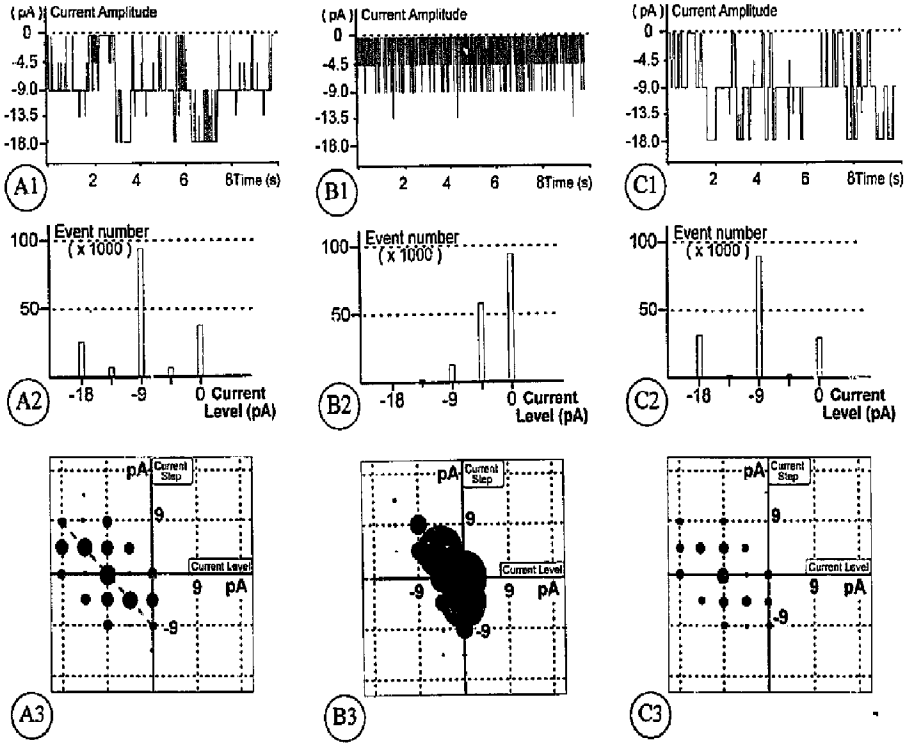

Fig. 5. Comparison of real data to different types of simulated signal data. (A1) Chloride channels signal of Fig. 3 after ideal reconstitution (1/80 point displayed). (A2) Classic current level histogram performed on an idealized real signal. The three main current levels (0, −9 and −18 pA) are shown as well as two intermediate sublevels (−4.5 and −13.5 pA). (A3) Event map of the idealized real signal. The time threshold is fixed to 0.5 ms. Consequently, short lasting event of less than 0.5 ms are plotted on abscissa axis as unresolved events. In this representation the five current levels are observed (vertical alignments at 0, −4.5, −9, −13.5 and −18 pA) as well as the four main current steps (horizontal alignments at ±4.5 pA and ±9 pA). ±9 pA current steps are missing at intermediate current levels (−4.5 and −13.5 pA). Unresolved events are more frequent at main current levels (0 pA, −9 pA and −18 pA). The figure exhibits a symmetry point (−9;0). (B1) Simulated signal of four independent subunits. Each subunit gating respects a Markovian process with $10^{-2}\ s^{-1}$ as opening rate constant and $7 \cdot 10^{-2}\ s^{-1}$ as closing rate constant. (B2) Current level histogram of the simulated signal B1. Peak distribution fits a binomial distribution ($P < 0.05$). Number of gating is regularly decreasing from fully closed state (four channels closed) to fully open state (four subunits open). As the opening rate constant is higher than the closing rate constant, the fully open state (−18 pA) is very rare. (B3) Event map of the signal B1. Distribution of current step is significantly different from this of real signal (Fig. 5-A3) ($P < 0.05$). (C1) Simulated signal built by the addition of two pairs of subunits exhibiting the cooperative model discribed in the Fig. 4. (C2) Current level histogram of the cooperative simulted signal of Fig. 5-C1. There is no statistical difference ($P < 0.05$) between this histogram and the histogram derived from real data (Fig. 5-A3). (C3) Event map of the cooperative simulated signal of Fig. 5-C1. The distribution of the events is statistically in agreement with the distribution of the corresponding events distribution observed for real data from the Fig. 5-A3 ($P < 0.05$).

TABLE I

Comparison between HUVEC chloride channel record and simulated cooperative tetrasubunit

Real data correspond to HUVEC chloride channels activity of a inside-out patch −40 mV clamped, with 110 mM TEACl, 10 mM Hepes in the pipette and in the bath. Simulated data correspond to a simulated tetrasubunit built with two pairs of cooperative subunits (kinetics described in Fig. 4). Duration of each record: 10 s. Sampling rate: 8 kHz. For each type of record, the number and the proportion of each current step between two consecutive current levels (*i* in pA) are reported. The comparison of current step distribution (χ^2: 13.54; threshold with $P < 0.05$ and 11 degrees of freedom: 19.67) shows no significant difference between real and simulated data.

Previous current level (pA)	0	0	−4.5	−4.5	−9	−9	−9	−9	−13.5	−13.5	−18	−18
Next current level (pA)	−4.5	−9	0	−9	0	−4.5	−13.5	−18	−9	−18	−9	−13.5
Current step amplitude (pA)	−4.5	−9	4.5	−4.5	−9	4.5	−4.5	−9	4.5	−4.5	9	4.5
Real data												
Number of steps	49	44	48	108	46	107	108	24	103	74	27	71
Percent of steps	6.1	5.4	5.9	13.3	5.7	13.2	13.3	3	12.7	9.1	3.3	8.8
Simulated data												
Number of steps	31	14	33	47	11	52	41	11	46	28	8	30
Percent of steps	8.8	4	9.4	13.4	3.1	14.8	11.6	3.1	13.1	8	2.3	8.5

coupling of gating between structural subunits of channel clusters. Furthermore, we are working on to know if the cooperativ model leads to a reinterpretation of the way classical Markov models have been used to analyse the data from other channels.

In this work, using an improved method of patch-clamp channel data analysis, we present evidence for the existence of four subunits of equal conductance (112.5 pS) in chloride channels of HUVEC. The observation of the event mapping and the analysis of the probabilities of occupancy of the different substates show that the behaviour of these channels deviates from a binomial distribution. A concerted model of two pairs of two subunits exhibiting a Markovian process is consistent with the experimental data. However, this model remains speculative and while useful conceptually to explain the data it may not in reality be the way these channels function since the ability of a model to reproduce data is not proof of a mechanism.

References

1 Hille, B. (1984) in Ionic channels of excitable membranes (Sunderland, M.A., ed.), Sinauer Associates.
2 Hamill, O.P., Marty, A., Neher, E., Sakmann, B. and Sigworth, F.J. (1981) Pflügers Arch. 391, 85–100.
3 Liebovitch, L.S., Fischbarg, J. and Koniarek, J.P. (1987) Math. Biosci. 84, 37–68.
4 Millhauser, G.L., Salpeter, E.E. and Oswald, R.E. (1988) Proc. Natl. Acad. Sci. USA 85, 1503–1507.
5 Millhauser, G.L. (1990) Biophys. J. 57, 857–864.
6 Liebovitch, L.S. and Toth, T.I. (1991) J. Theor. Biol. 148, 243–267.
7 Sansom, M.S., Ball, F.G., Kerry, C.J., McGee, R., Ramsey, R.L. and Usherwood, P.N. (1989) Biophys. J. 56, 1229–1243.
8 McManus, O.B., Weiss, D.S., Spivak, C.E., Blatz, A.L. and Magleby, K.L. (1988) Biophys. J. 54, 859–870.
9 McManus, O.B., Spivak, C.E., Blatz, A.L., Weiss, D.S. and Magleby, K.L. (1989) Biophys. J. 55, 383–385.
10 Liebovitch, L.S. and Toth, T.I. (1990) Synapse 5, 134–138.
11 Fox, J.A. (1987) J. Membr. Biol. 97, 1–8.
12 Miller, C. (1982) Phil. Trans. R. Soc. Lond. Biol. 299, 401–411.
13 Geletyuk, V.I. and Kazachenko, V.N. (1985) J. Membr. Biol. 86, 9–15.
14 Sauve, R., Roy, G. and Payet, D. (1983) J. Membr. Biol. 74, 41–49.
15 Takeda, K. and Trautmann, A. (1984) J. Physiol. Lond. 349, 353–374.
16 Weik, R., Lonnendonker, U. and Neumcke, B. (1989) Biochim. Biophys. Acta 983, 127–134.
17 Hamill, O.P., Bormann, J. and Sackmann, B. (1983) Nature 305, 805–808.
18 Hunter, M. and Giebisch, G. (1987) Nature 327, 522–524.
19 Auerbach, A. and Sachs, F. (1983) Biophys. J. 42, 1–10.
20 Fishman, H.M., Leuchtag, H.R. and Moore, L.E. (1983) Biophys. J. 43, 293–307.
21 Neumcke, B. and Stampfli, R. (1983) Biochim. Biophys. Acta 727, 177–184.
22 Horn, R. (1984) in Ion Channels: Molecular and Physiological Aspects (Stein, W.D., ed.), pp. 53–97, Academic Press, New York.
23 Kiss, T. and Nagy, K. (1985) Eur. Biophys. J. 12, 13–18.
24 Fishman, H.M. (1985) Prog. Biophys. Mol. Biol. 46, 127–162.
25 Jaffé, E.A., Nachman, R.L., Becker, C.G. and Minick, C.R. (1973) J. Clin. Invest. 52, 2745–2756.
26 Sigworth, F.J. (1983) Single-Channel Recording (Sakmann, B. and NEHER, E., eds.), pp. 301–321, Plenum Press, New York.
27 Nilius, B. (1990) Pflügers Arch. 416, 609–611.
28 Bossu, J.L., Feltz, A., Rodeau, J.L. and Tanzi, F. (1989) FEBS Lett. 255, 377–380.
29 Takeda, K., Schini, V. and Stoeckel, H. (1987) Pflügers Arch. 410, 385–393.
30 Queyroy, A., Tranqui, L. and Verdetti, J. (1991) J. Mol. Cell. Cardiol. 23 (Suppl. I), 151(Abstr.).
31 Barrett, J.N., Magleby, K.L. and Pallotta, B.S. (1982) J. Physiol. Lond. 331, 211–230.
32 Meeves, H. and Nagy, K. (1989) Biochim. Biophys. Acta 988, 99–105.
33 Stockbridge, L.L., French, A.S. and Man, S.F. (1991) Biochim. Biophys. Acta 1064, 212–218.
34 Bosma, M.M. (1989) J. Physiol. Lond. 410, 67–90.

35 Liebovitch, L.S. and Sullivan, J.M. (1987) Biophys. J. 52, 979–988.
36 Fishman, H.M., Leuchtag, H.R. and Poussart, D. (1984) Biophys. J. 45, 46–49.
37 Hill, T.L. and Chen, Y.D. (1971) Proc. Natl. Acad. Sci. USA 68, 2488–2492.
38 Chapron, Y., Cochet, C., Crouzy-S., Jullien, T., Keramidas, M. and Verdetti, J. (1989) Biochem. Biophys. Res. Commun. 158, 527–533.
39 Changeux, J.P., Giraudat, J. and Dennis, M. (1987) Trends Pharmacol. Sci. 8, 459–465.
40 Morris, C.E. and Montpetit, M. (1986) Can. J. Physiol. Pharmacol. 64, 347–355.
41 Cull-Candy, S.G. and Usowicz, M.M. (1989) J. Physiol. Lond. 415, 555–582.
42 Prod'hom, B., Pietrobon, D. and Hess, P. (1987) Nature 329, 243–246.
43 Monod, J., Wyman, J. and Changeux, J.P. (1965) J. Mol. Biol. 12, 88–118.